Triazinium Ligation: Bioorthogonal Reaction of *N*1-alkyl 1,2,4-Triazinium Salts

Veronika Šlachtová,[1] Simona Bellová,[1] Agustina La-Venia,[1,2] Juraj Galeta,[1] Martin Dračínský,[1] Karel Chalupský,[1] Helena Mertlíková-Kaiserová,[1] Peter Rukovanský,[1] Rastislav Dzijak[1] and Milan Vrabel*[1]

[1] Institute of Organic Chemistry and Biochemistry of the Czech Academy of Sciences, Flemingovo nám. 2, 16000, Prague (Czech Republic)

[2] Current address: Instituto de Química Rosario, Facultad de Ciencias Bioquímicas y Farmacéuticas, Universidad Nacional de Rosario-CONICET, Suipacha 531, S2002LRK, Rosario, Argentina

KEYWORDS: Bioorthogonal, click reactions, 1,2,4-triazines, protein labeling, bioimaging, IEDDA

ABSTRACT: The development of reagents that can selectively react in complex biological media is an important challenge. Here we show that *N*1-alkylation of 1,2,4-triazines yields the corresponding triazinium salts, which are three orders of magnitude more reactive in reactions with strained alkynes than the parent 1,2,4-triazines. This powerful bioorthogonal ligation enables efficient modification of peptides and proteins. The positively charged *N*1-alkyl triazinium salts exhibit favorable cell permeability, which makes them superior for intracellular fluorescent labeling applications when compared to analogous 1,2,4,5-tetrazines. Due to their high reactivity, stability, accessibility and improved water solubility, the new ionic heterodienes represent a valuable addition to the repertoire of existing modern bioorthogonal reagents.

INTRODUCTION

Chemical reactions compatible with biological systems have numerous applications. They are employed in the modification of biopolymers,[1-3] the visualization of small molecules and biomolecules inside cells[4-5] and also in biomedicine.[6-7] To proceed efficiently and selectively, the reagents involved in these reactions must be sufficiently reactive and stable in biological media. In recent decades, numerous biocompatible reagents and reactions have been developed.[8-10] Among these, various strain-driven cycloadditions have become popular for their ability to proceed cleanly and selectively (even in a crowded biological environment) without the need for an additional catalyst. For example, the strain-promoted azide-alkyne cycloaddition (SPAAC)[11-12] and its variations employing other dipoles[13-15] have found application in a wide range of fields. Another popular cycloaddition is the inverse electron-demand Diels-Alder reaction (IEDDA) of 1,2,4,5-tetrazines with strained dienophiles.[16-18] Although a number of strained olefins have been developed as reaction partners in IEDDA,[19-23] there are far fewer examples of dienes that can be used in this reaction. Besides 1,2,4,5-tetrazines, derivatives of 1,2,4-triazines have been developed as more stable alternatives.[24-26] However, the improved stability of triazines is associated with reduced reaction rates.

Due to the inverse electron demand characteristic of IEDDA, the attachment of electron-withdrawing substituents to the heterocyclic core enhances the reactivity of the dienes in the cycloaddition. This strategy has been successfully utilized to improve the reactivity of both, 1,2,4-triazines[24, 27] and 1,2,4,5-tetrazines.[28] However, especially for tetrazines, these modifications also increase the susceptibility to nucleophilic attack at the electron-deficient positions 3- and 6-, which can lead to their degradation in biological media.[29] Therefore, there is a growing demand for new strategies that increase the reactivity of bioorthogonal reagents without reducing their stability.

Recently, a distortion caused by a repulsive N-O interaction of vinyl ether-substituted tetrazines was described as a strategy to increase their reactivity without impeding their stability.[30] Another elegant solution for generating highly reactive tetrazines is based on light-triggered photoactivation of stable dihydrotetrazine precursors.[31-32] More recently, dihydrotetrazines modified with photocaging groups as precursors to 1,2,4,5-tetrazines have been proposed (Figure 1).[33] In spite of these advances, the development of highly reactive and at the same time stable bioorthogonal reagents remains challenging. Moreover, similar strategies for 1,2,4-triazines have yet to emerge.

Two other important parameters, especially for intracellular application of bioorthogonal reactions, are the solubility and cell permeability of the reagents. Water solubility is typically enhanced by the attachment of polyethylene glycol (PEG) linkers of various length to molecules. However, this increases the molecular weight of the compounds, which can influence their (bio)distribution, impede their ability to cross cell membranes and even cause an immune reaction.[34] An alternative strategy involves the modification of molecules by charged moieties, such as sulfo groups. Indeed, a number of commercial tetrazine derivatives contain sulfo groups, e.g. sulfonated dyes.

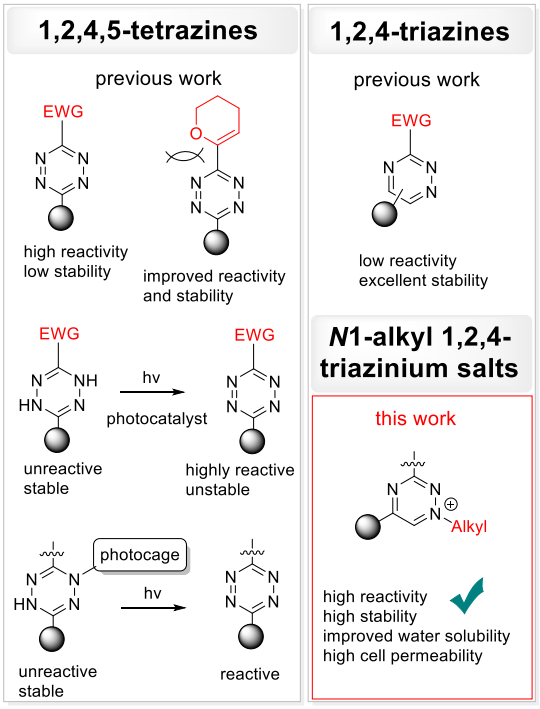

Figure 1. Previous and new strategies for improving the reactivity and stability of heterodienes in bioorthogonal reactions.

However, these effectively render compounds cell-impermeable, which limits their use mainly to fixed and permeabilized cells. By contrast, the introduction of positive charge(s), which can significantly enhance the water solubility and cell permeability of molecules,[35] is much less common. Previously, we demonstrated that the attachment of a charged pyridinium moiety to 1,2,4-triazines yields a notable group of water-soluble, cell-permeable compounds with enhanced applicability in bioconjugations.[27] More recently, we extended this approach to positively-charged mitochondriotropic tetrazines, which can activate *trans*-cyclooctene-caged prodrugs in an organelle-specific manner.[36] These examples indicate that positively charged groups can endow molecules with advantageous properties. Yet, in the context of bioorthogonal reagents, these effects remain largely unexplored.

In this work, we show that selective alkylation of 1,2,4-triazines at nitrogen *N*1 yields the corresponding *N*1-alkyl triazinium salts (**Trz$^+$s**), which are not only stable under biological conditions, but also highly reactive in reaction with strained alkynes. In addition, the compounds have improved water solubility while displaying high cell-permeability (Figure 1). A head-to-head comparison of the triazinium salts with the popular 1,2,4,5-tetrazines shows that the new reagents outperform the latter compounds in intracellular labeling experiments. As we demonstrate in several examples, these features make **Trz$^+$s** expedient bioorthogonal reagents in a wide range of applications, from selective peptide and protein labeling to cellular imaging.

RESULTS AND DISCUSSION

We and others have previously used triazinium salts as precursors to the corresponding triazinium ylides, which are formed in situ under basic conditions. These dipoles react in 1,3-dipolar cycloadditions with electron poor dipolarophiles to yield pyrrolotriazines.[37-38] Alternatively, an intramolecular cycloaddition of triazinium salts leading to substituted pyridines has been described.[39] In this context, we sought to exploit triazinium salts as chemoselective reaction partners in bioorthogonal cycloadditions with strained dienophiles. To this end, we carried out a reaction of *N*1-methyl-3,5-diphenyl triazinium (**Trz$^+$1**) with *endo*-bicyclo[6.1.0]non-4-yn-9-ylmethanol (***endo*-BCN**) (Figure 2A). Upon mixing the reagents, we observed a clean conversion to the corresponding pyridine cycloadduct **1** within a couple of minutes (Figure 2B). Compared with the non-alkylated 3,5-diphenyl-1,2,4-triazine (**Trz1**), the reaction of **Trz$^+$1** with ***endo*-BCN** was three orders of magnitude faster (k_2 = 0.021 M^{-1} s^{-1} and 20 M^{-1} s^{-1}, respectively). This result shows that alkylation of the triazine heterocycle at nitrogen *N*1 induces a dramatic increase in reactivity. Notably, alkylation of 3,6-diphenyl-1,2,4,5-tetrazine (**diPhTz**) under the same conditions was unsuccessful, resulting only in the isolation of the corresponding reduced dihydrotetrazine. By contrast, alkylation of 3,6-diphenyl-1,2,4-triazine was successful, despite the ensuing click ligation with ***endo*-BCN** generating a complex mixture of products (SI).

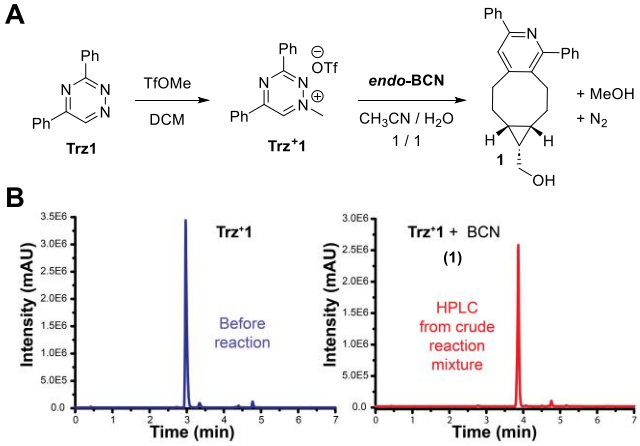

Figure 2. (A) Methylation of 3,5-diphenyl-1,2,4-triazine produces *N*1-methyl-1,2,4-triazinium salt that efficiently reacts with strained ***endo*-BCN** alkyne. (B) HPLC chromatograms show clean conversion of **Trz$^+$1** in reaction with ***endo*-BCN** giving rise to the corresponding cycloaddition product.

To understand the basis for the increased reactivity of 3,5-disubstituted *N*1-alkyl triazinium salts, we performed a computational study at the density-functional-theory (DFT) level. We found transition-state (TS) structures for the IEDDA reaction of ***endo*-BCN** with **Trz1** and with **Trz$^+$1**. The relative free energy of the TS with the triazinium derivative was 10 kcal mol^{-1} lower than that of the TS with the triazine starting compound (Figure 3A), which confirms strong preference of ***endo*-BCN** to react with the positively charged heterodiene.

The subsequent reaction steps after formation of the cycloaddition product involve either denitrogenation of the

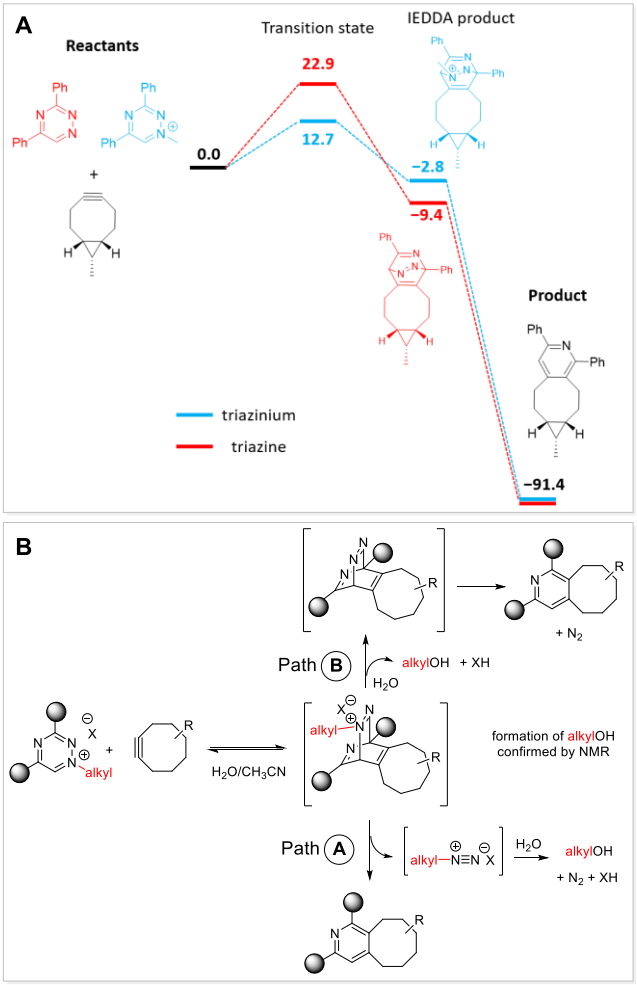

Figure 3. (A) The calculated (B3LYP/6-31+G(2d,p)/CPCM) relative free energies (kcal mol^{-1}) of the reactants, transition-state structures and products of the IEDDA reaction of **Trz1** and **Trz$^+$1** with ***endo*-BCN** (the hydroxymethyl group was substituted with a methyl group for simplification). (B) Proposed reaction mechanism of the triazinium ligation.

triazine intermediate or the departure of the alkyl diazonium species from the triazinium intermediate followed by hydrolysis to give an alcohol and a nitrogen molecule (Path A in Figure 3B). Alternatively, we speculate that hydrolysis may precede the denitrogenation step (Path B in Figure 3B). While evolution of nitrogen gas (bubbling) during the reaction was observed experimentally, presence of the hydrolysis product (an alcohol) was confirmed by NMR spectroscopy (Figure S2 in the SI). Computational analysis of the reactions following the formation of the IEDDA product showed both to be low-barrier processes (SI). Therefore, we could not unambiguously rule out or confirm any of the routes.

Based on these preliminary data, we next investigated how the different alkyl groups would affect the reactivity, solubility, and stability of the triazinium ions. Methylated and ethylated derivatives are synthetically accessible via alkylation by commercial methyl- and ethyl-trifluoromethanesulfonates.[38] For preparation of *iso*-propyl (*i*Pr) and *tert*-butyl (*t*Bu) analogs, we generated the corresponding triflates in situ from the respective alcohols and triflic acid anhydride in the presence of pyridine (SI).

Second order rate constants for all derivatives were determined in a CH_3CN/H_2O (1:1) mixture at room temperature using an excess of ***endo*-BCN**. These measurements showed that the reactivity decreased, while the size of the alkyl substituent in the series Me vs Et vs *i*Pr increased (Figure 4A and Table S6 in the SI). Surprisingly, **Trz$^+$4** containing the bulky *t*Bu group was found to be most reactive. Since it is also the most lipophilic derivative, the increase in reactivity may be attributed, at least in part, to the increased hydrophobicity effect.[40] Interestingly, all triazinium salts proved more reactive than **diPhTz** in reaction with ***endo*-BCN**. This was also confirmed in a competition experiment, where an equimolar amount of **Trz$^+$4** and **diPhTz** was treated with one equivalent of ***endo*-BCN**. This experiment revealed that 3.4-times more of the triazinium click product was formed in the reaction mixture (Figure S13 in the SI).

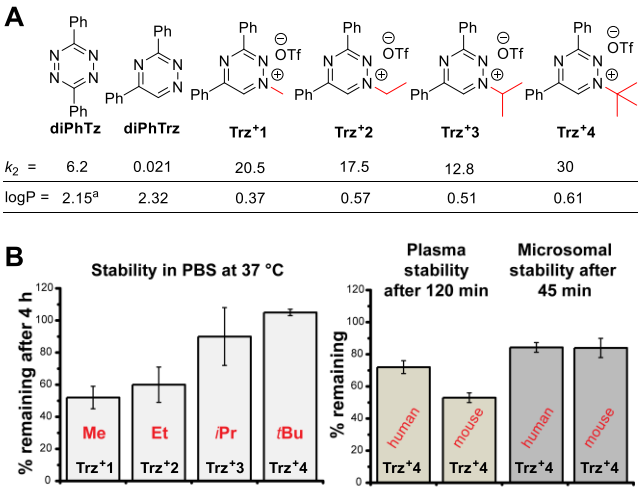

Figure 4. (A) Second-order rate constants (in M^{-1} s^{-1}) for the reactions of **diPhTz**, **diPhTrz**, and differently alkylated triazinium salts with ***endo*-BCN** determined in a CH_3CN/H_2O (1:1) mixture at room temperature; experimentally determined logP values are also given. [a]This logP value was calculated using StarDrop software due to very low solubility in the water/octanol mixture. (B) Stability of differently alkylated triaziniums in PBS at 37 °C and stability of **Trz$^+$4** in the plasma and microsomes of humans or mice.

The logP values increased with the steric bulk of the alkyl group, but fell well below those of the corresponding **diPhTrz** or **diPhTz** (Figure 4A). These data confirm the enhanced water solubility of the triazinium compounds. Further calculated and experimental logP values can be found in the SI.

During initial experiments, we noted that the solvent had a significant effect on the stability of the compounds. While all derivatives were stable for 4 hours in water (Figure S15 in the SI), Me-, Et-, and *i*Pr-substituted triaziniums partially decomposed over the course of 4 hours in phosphate-buffered saline (PBS) when incubated at 37 °C (Figure 4B). The only exception was the *t*Bu analog, which was perfectly stable even in PBS. In fact, ca. 80% and 70% of **Trz$^+$4** remained intact even in full cell growth medium (Dulbec-

co's Modified Eagle Medium (DMEM) containing 10% fetal bovine serum) when incubated at 37 °C for 24 and 48 hours, respectively (Figure S17 in the SI). Additional plasma and microsomal stability (human and mouse) measurements corroborated the superior stability of the compound (Figure 4B). Together, these data clearly indicate that *t*-butylated triazinium salts are the most suitable compounds for further study.

Our initial *t*-butylation procedure used for preparing **Trz⁺4** based on alkylation of **diPhTrz** by in situ-generated *t*Bu-triflate proved poorly reproducible. To ensure synthetic access to the compounds, we optimized this crucial step by investigating a number of reaction conditions and different alkylating agents (SI). This led to the identification of isobutene, which in the presence of triflic acid in DCM, led to clean and regioselective alkylation at nitrogen *N*1 in a 95% yield (Figure 5A). Importantly, when the alkylation reaction was successfully performed on a larger scale (2.5 g), the product was still isolated in an 80% yield (SI).

After successfully establishing synthetic access to the compounds, we next studied the effect of different counterions on the solubility of di-phenyl-substituted *t*-butylated triazinium salts. Solubility in PBS at pH=7.4 was around 90 µM and is similar for $CF_3SO_3^-$, CF_3COO^- and Cl^- counterions despite the different logP values of the triazinium salts (Table S11 in the SI). Surprisingly, we observed differences in the reactivity of triaziniums bearing different counterions, of which the **Trz⁺4** (**$CF_3SO_3^-$**) salt was the most reactive (Table S7 in the SI).

Using the optimized alkylation procedure, we prepared a small series of **Trz⁺s** bearing electron-withdrawing or -donating groups (**Trz⁺5** - **Trz⁺8**) at positions 3 or 5 of the phenyl ring to investigate the influence of substituents on the click reaction rate with ***endo*-BCN** (Figure 5A and 5B). As expected, introducing an electron donating methoxy-phenyl group (**Trz⁺5**) at position 5 resulted in deceleration relative to diphenyl-substituted **Trz⁺4** (57 M^{-1} s^{-1} vs 100 M^{-1} s^{-1}). By contrast, the presence of an electron-withdrawing CF_3-phenyl group at the same position increased the reactivity of **Trz⁺6** (127 M^{-1} s^{-1}). Surprisingly, modification of the phenyl ring at position 3 by electronically different substituents decreased the reactivity and yielded rate constants of 52 M^{-1} s^{-1} and 64 M^{-1} s^{-1} for **Trz⁺7** and **Trz⁺8**, respectively.

To test the potential for **Trz⁺s** to be used in combination with other dienophiles, we measured the reaction kinetics of **Trz⁺4** with ***exo*-BCN** isomer, the less strained cyclooct-2-yn-1-ol (**SCO**) and dibenzocyclooctyne acid (**DBCO-acid**) (Figure 5C). The difference in reactivity between the two **BCN** isomers with **Trz⁺4** was small (100 M^{-1} s^{-1} vs 108 M^{-1} s^{-1}). In contrast, **SCO** reacted two orders of magnitude slower (2 M^{-1} s^{-1}), which is in the range of reactivity exhibited by, e.g., tetrazines with norbornenes.[20] Interestingly, we isolated a single regioisomer from the reaction of **SCO** with **Trz⁺4**. This offers the possibility of preparing defined ligation products using this dienophile. On the other hand, we did not observe any reaction of **Trz⁺4** with **DBCO-acid**. This might be attributed to increased steric demand in the transition state, as in the case of 1,2,4,5-tetrazines.[41] Investigation of other dienophiles as reaction partners in the triazinium ligation, such as derivatives of norbornenes,

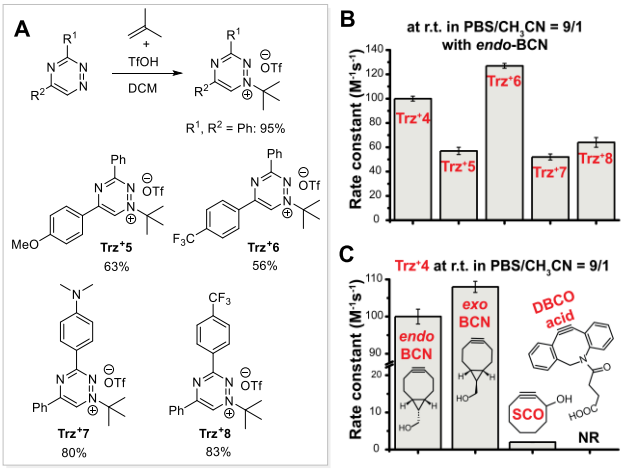

Figure 5. (A) Optimized *t*-butylation of 1,2,4-triazines using isobutene and triflic acid was used for the synthesis of a series of triazinium triflates (yields of isolated compounds are shown). (B) Graph shows second-order rate constants of reactions between differently substituted triaziniums and ***endo*-BCN**. (C) Graph shows second-order rate constants for reactions between **Trz⁺4** and various dienophiles. r.t. = room temperature, NR = no reaction.

cyclopropenes or *trans*-cyclooctenes is currently under investigation in our lab.

Various mutually orthogonal biocompatible reactions are becoming increasingly popular as they provide an opportunity to analyze complex biological events simultaneously.[42-43] Given that **Trz⁺4** did not react with **DBCO-acid**, we decided to explore the possibility of using triazinium ligation in combination with the SPAAC reaction (Figure 6). In the first experiment, we mixed equivalent amounts of 3-azido-coumarin (**Az-Coum**), **Trz⁺4**, and **DBCO-acid** in a CH_3CN/H_2O (1:1) mixture and incubated the reagents for 1 hour at room temperature. After this time, HPLC-MS analysis showed only a selective SPAAC reaction between **Az-Coum** and **DBCO-acid**, indicating that neither azide nor DBCO reacted with the triazinium (Figure S22 in the SI). To explore the selectivity further, we mixed an equimolar amount of **Az-Coum** and **Trz⁺4** with one equivalent of ***endo*-BCN**. In this case, the azide and triazinium competed for the strained alkyne. Due to the much higher reactivity of ***endo*-BCN** with **Trz⁺4** compared with the azide, HPLC-MS recorded a signal corresponding almost exclusively to the triazinium click ligation product as early as in 30 min after the experiment. Only traces of the corresponding SPAAC product arising from the reaction of **Az-Coum** with ***endo*-BCN** were detected in the chromatogram (Figure S23 in the SI). Finally, we performed the experiment with all four reagents by combining pre-mixed solutions of **Az-Coum** and **Trz⁺4** with ***endo*-BCN** and **DBCO-acid**. After 30 min, HPLC-MS analysis confirmed a selective reaction of **Trz⁺4** with ***endo*-BCN** and of **DBCO-acid** with **Az-Coum**. Only traces of the SPAAC product between **Az-Coum** and ***endo*-BCN** were detected (Figure 6 and S24). These data indicate that triazinium ligation is orthogonal to the popular SPAAC reaction, making this conjugation a valuable addition to the repertoire of mutually orthogonal biocompatible reactions.

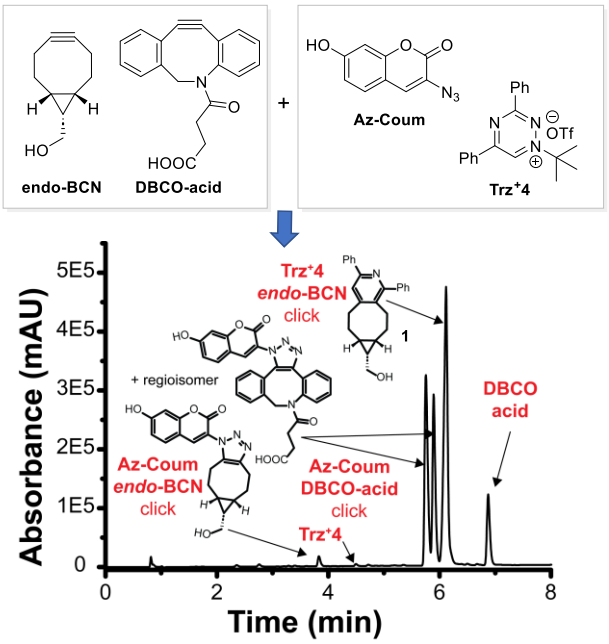

Figure 6. Mutually orthogonal click reaction experiment. An equimolar amount of ***endo*-BCN** and **DBCO-acid** was combined with an equimolar amount of **Az-Coum** and **Trz⁺4** in a CH_3CN/H_2O (1:1) mixture at room temperature. HPLC-MS analysis of the crude reaction mixture performed after 30 min revealed highly selective formation of SPAAC and triazinium click ligation products. Additional experiments can be found in the SI.

Labeling and modification of biomolecules are important applications of bioconjugations. To investigate the extent of selectivity and efficiency of the triazinium ligation when performed on biomolecules, we first prepared a BCN-containing peptide (**BCN-peptide**)[44] and mixed it with **Trz⁺4**. The reagents were incubated for 30 min in a CH_3CN/H_2O (1:1) mixture at room temperature. The reaction proceeded cleanly and selectively, and the expected click peptide was formed in full conversion (Figure 7A and S25 in the SI).

To study the new triazinium ligation on a protein, we performed the reaction with ADP-ribosylation factor 1 (**Arf1**).[45] First, the single cysteine residue of **Arf1** was modified with the commercial **SCO-PEG$_3$-maleimide** to yield **Arf1-SCO** (SI). After gel filtration, we added **Trz⁺4** (10 equiv.) to **Arf1-SCO** and incubated the mixture for 2 hours at room temperature. After that, intact protein mass analysis of the reaction mixture revealed successful formation of the click-labeled product without any traces of the starting protein (Figure 7B). Importantly, we did not observe any modification or side reactions in the control experiment, where unmodified **Arf1** protein was incubated under the same conditions with **Trz⁺4** (Figure S26 in the SI). This result indicates that the reaction depends on the presence of the strained alkyne and that it is selective even in the presence of other functional groups in the side chains of amino acids. These experiments highlight the favorable selectivity and efficiency of the triazinium ligation and its application potential for labeling biomolecules.

To demonstrate that the triazinium click group can be embedded into structurally more complex molecules, we prepared a series of derivatives bearing various functional moieties (Figure 7C). These included an *N*-hydroxysuccinimide (NHS) active ester (**Trz⁺9**) for modification of amino group-containing molecules (e.g., small molecules, peptides, or proteins), an amino group (**Trz⁺10**) for peptide couplings, arylpropionitrile (APN) for conjugation to cysteine residues (**Trz⁺11**), biotin for pull-down or western blot analysis (**Trz⁺12**), and various dye conjugates for bioimaging applications (**Trz⁺13 - 15**). The latter derivatives are synthetically accessible by late-stage functionalization of **Trz⁺9** and **Trz⁺10** (SI).

Labeling and visualization of molecules in living cells are among the most challenging applications of bioorthogonal reactions.[4] Accordingly, we analyzed the triazinium ligation in this complex environment. To compare the new reagents with the more established 1,2,4,5-tetrazines, we used a set of analogous compounds bearing this heterodiene. In the first experiment, we performed the reaction on living cells treated with BCN-modified concanavalin A (**BCN-ConA**), a lectin with high specificity for α-D-mannose and α-D-glucose residues.[46] In the control experiment, cells were treated in the same manner but with unmodified **ConA**. U2OS osteosarcoma cancer cells pretreated with the lectin were washed and incubated with 10 μM **Trz⁺14** or the analogous **MeTz-AF488** for 1 hour. After washing, cells were inspected on a confocal microscope. Under these conditions, both reagents provided a clean labeling pattern on the cell surface (Figure 8A and 8C and Figure S27 in the SI). We did not observe any labeling in control experiments when cells were pre-treated with the unmodified **ConA** (Figure 8B and 8D). These data show that the new triazinium ligation is comparable to the popular tetrazine ligation in enabling efficient labeling of BCN-modified proteins on living cells.

To further evaluate the triazinium reagents, we performed the reaction inside living cells. In this experiment, we used a BCN-triphenylphosphonium conjugate (**BCN-TPP**), which we previously employed in intracellular fluorescence turn-on labeling studies.[47] The TPP moiety is known to target small molecules to mitochondria thus ensuring the construct remains inside the cells.[48] We compared the new triazinium reagents with the corresponding tetrazines in this case as well. Living HeLa cells were treated with **BCN-TPP** for 10 min and subsequently washed to remove any extracellular compound. Next, the click reagents conjugated to the cell-permeable coumarin dye (**Trz⁺13** and **MeTz-Coum**) were added to the cells at a low 1 μM concentration and were incubated for 30 min. The cells were washed and inspected on a confocal microscope. In contrast to **Trz⁺13**, which showed clear labeling inside the cells (Figure 8E), we did not observe any labeling with the corresponding tetrazine reagent at this concentration. Increasing the concentration 5-fold did not improve the results (Figure S28 in the SI). Finally, 10 μM of **MeTz-Coum** yielded weak, but visible signal inside the cells (Figure 8G). We assumed the lower reactivity of the methyl tetrazine was responsible for the reduced intensity of the labeling.[49] Therefore, we performed the same experiment, but this time used the corresponding coumarin probe containing the more reactive H-tetrazine (**HTz-Coum**).

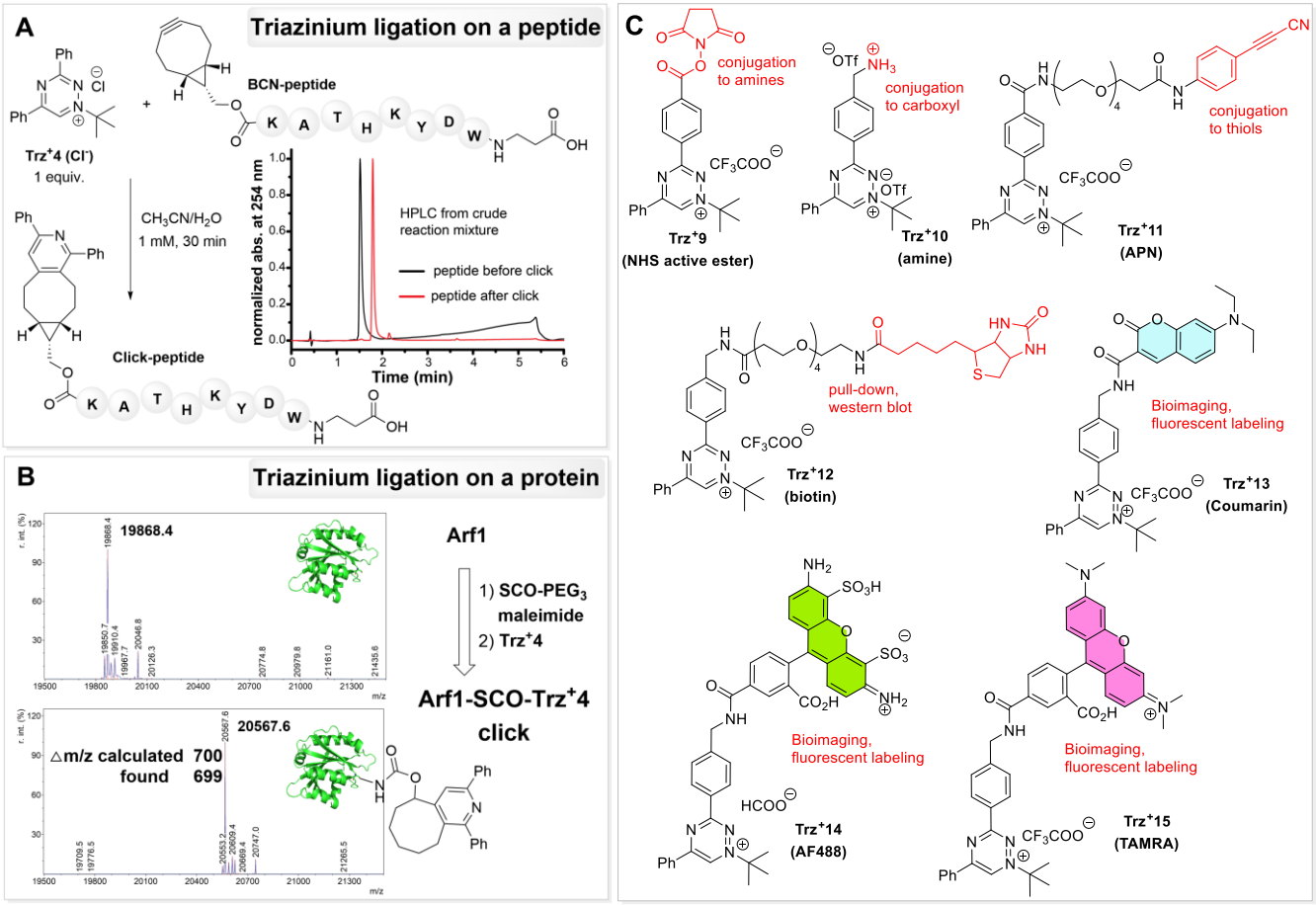

Figure 7. Triazinium ligation was used to label (A) model peptide and (B) the protein Arf1. (C) Examples of triazinium derivatives bearing different functional moieties useful for various synthetic and biological applications.

Surprisingly, even the use of **HTz-Coum** did not result in efficient labeling in cells at 1 μM concentration (Figure S28 in the SI). However, increasing the concentration of **HTz-Coum** to 5 μM and then to 10 μM led to the formation of a visible signal inside the cells (Figure 8H). We also quantified the labeling efficiency of the individual compounds by fluorescence-assisted cell sorting (FACS) analysis, which confirmed the data obtained from confocal microscopy (Figure S29 in the SI).

Perhaps surprisingly, the reactivity of bioorthogonal reagents is not the sole determinant of their performance inside living cells. We and others have observed that cell permeability and stability of compounds are equally important parameters.[50-52] To explain the enhanced intracellular labeling observed for the triazinium salt, we incubated cells with all three compounds: **Trz⁺13**, **MeTz-Coum** and **HTz-Coum**. We then briefly washed the cells, and quantified intracellular fluorescence intensity by FACS. This analysis revealed that larger amount of the charged triazinium was present inside the cells compared with the tetrazines (Figure 8J). This result can be attributed to the enhanced cell permeability of compound **Trz⁺13**, which differed from the respective tetrazines only in the heterodiene part.

We also speculated whether the potential fluorogenic properties of the probes would contribute to the observed differences in labeling. Based on measurements of the fluorescence spectra of the coumarin-containing probes before and after the reaction with ***endo*-BCN** all three compounds exhibited fluorogenic properties. However, there were no significant differences (Figure 8K). Surprisingly, we observed turn-on in fluorescence even after the reaction of **Trz⁺13** with the dienophile, which suggests that triazinium salts could serve as a new fluorescence quenching moiety.

To rule out the possibility that the observed enhanced labeling was limited to the mitochondrial **BCN-TPP** probe, we performed analogous experiments with **BCN-PEG₃-amine.**[52] These results proved similar, corroborating the higher labeling efficacy of **Trz⁺13** at 1 μM concentration in comparison with **MeTz-Coum** and **HTz-Coum** (Figure S30 and 31 in the SI). The increased labeling efficiency inside living cells can be attributed mainly to the increased cellular permeability of the compounds involved. Importantly, these new triazinium salts are not toxic under these conditions at least for the four cell lines tested (Figure S36 and Table S12 in the SI). Our experiments clearly demonstrate the superior properties of these new triazinium probes for intracellular labeling applications, where they outperform even the popular tetrazines.

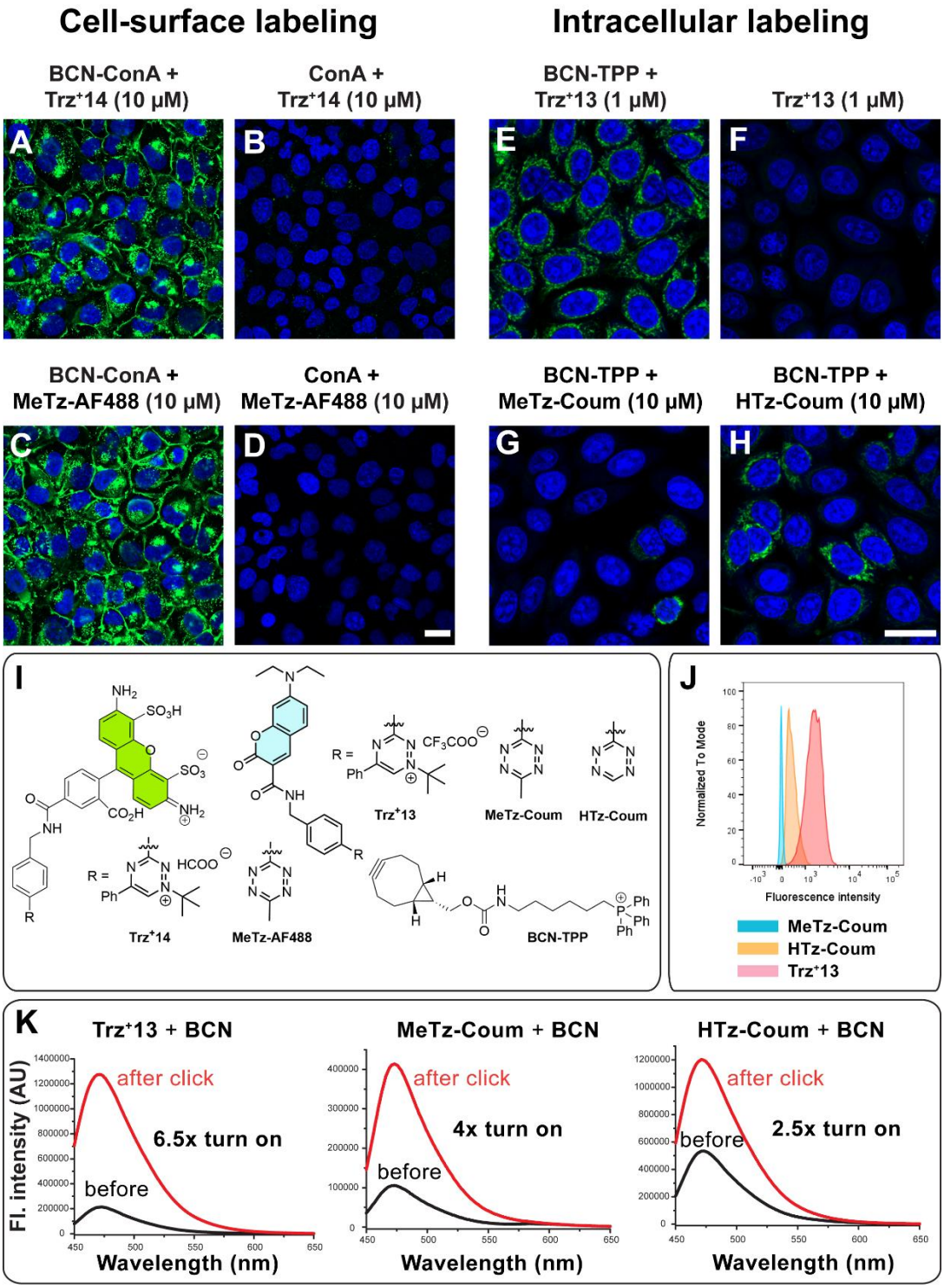

Figure 8. Comparison of triazinium and tetrazine ligations in bioimaging experiments. Cell surface labeling: living U2OS cells were treated with **BCN-ConA** or **ConA** as a control and subsequently with **Trz⁺14** and **MeTz-AF488** (10 µM for 1 hour). Cells were washed with cell medium before imaging. (A) Labeling with **Trz⁺14** and (B) the corresponding control experiment with **ConA**. (C) Labeling with **MeTz-AF488** and (D) the corresponding control experiment with **ConA**. The click labeling signal is shown in green. Cell nuclei were stained with Hoechst 33342 dye shown in blue. Intracellular labeling: living HeLa cells were treated with **BCN-TPP** (5 µM for 10 min) and subsequently for 30 min with (E) **Trz⁺13** (1 µM), (F) only with **Trz⁺13** (1 µM), (G) with **MeTz-Coum** (10 µM) or (H) with **HTz-Coum** (10 µM). Cells were washed twice before imaging. Further experiments performed at different concentrations and control experiments can be found in the SI. Cell nuclei were stained with DRAQ5 dye shown in blue. Scale bar is 25 µm. (I) Structures of the reagents. (J) FACS analysis of cells treated with **MeTz-Coum**, **HTz-Coum** and **Trz⁺13** (1 µM for 30 min) demonstrate the enhanced cell permeability of triazinium reagent. (K) Fluorescence spectra of the reagents before and after the reaction with ***endo*-BCN** highlight the fluorogenic properties of the compounds.

CONCLUSIONS

In this work, we introduce a new bioorthogonal conjugation, triazinium ligation, which is based on the reaction of *N*1-alkyl 1,2,4-triazinium salts with strained alkynes. The key triazinium reagents are readily accessible via optimized alkylation of 1,2,4-triazines, enabling access to derivatives with tunable reaction rates. Alkylation accelerates the reaction by three orders of magnitude compared with the parent triazines. The enhanced reactivity of the salts is caused by the lower relative free energy of the corresponding transition state, as revealed by DFT calculations. From among the alkylated derivatives, *tert*-butylation was the modification of choice as the corresponding triazinium salts proved both, highly reactive and stable in a biological milieu. The triazinium ligation is orthogonal to the strain-promoted azide-alkyne cycloaddition, which should allow these two reactions to be performed on a single system. We demonstrate that this new conjugation can be used for clean and efficient modification of biomolecules such as peptides and proteins. According to our comparative cell-labeling study, the increased cell permeability of the positively charged triazinium salts enhanced the efficiency of intracellular labeling compared with analogous tetrazine derivatives. Based on the data presented here, we expect triazinium ligation to become a valuable addition to existing bioconjugations, and that this chemical reaction will further expand the application potential of bioorthogonal transformations in chemical biology and beyond.

ASSOCIATED CONTENT

Supporting Information. Synthetic procedures, characterization data of all new compounds, kinetic measurements, compound stability studies, additional cellular experiments and cytotoxicity measurements. This material is available free of charge via the Internet at http://pubs.acs.org."

AUTHOR INFORMATION

Corresponding Author

* **Milan Vrabel** – Institute of Organic Chemistry and Biochemistry of the Czech Academy of Sciences, Flemingovo nám. 2, 160 00, Prague, Czech Republic, Phone: +420 220 183 317, E-mail: vrabel@uochb.cas.cz.

Author Contributions

All authors contributed to the performance of the study and the writing of the manuscript, and have approved the final version for publication.

Notes

The authors declare no competing interests.

ACKNOWLEDGMENT

This work was supported by the Academy of Sciences of the Czech Republic (RVO: 61388963), the Czech Science Foundation (P207/20-30494L) and the National Institute for Research of Metabolic and Cardiovascular Diseases (Programme EXCELES, ID Project No. LX22NPO5104) - Funded by the European Union – Next Generation EU. V. S. is grateful for support from the IOCB postdoctoral fellowship. We wish to thank Prof. Pavel Kočovský for critical reading of the manuscript, Michael FitzGerald for language corrections, the Department of Mass Spectrometry at IOCB for measurement of the intact protein masses, the group of Biochemical pharmacology at IOCB, and Jana Günterová for help with the flow cytometry analysis.

REFERENCES

(1) Lallana, E.; Riguera, R.; Fernandez-Megia, E. Reliable and efficient procedures for the conjugation of biomolecules through Huisgen azide-alkyne cycloadditions. *Angew. Chem. Int. Ed. Engl.* **2011,** *50* (38), 8794-8804.

(2) Takaoka, Y.; Ojida, A.; Hamachi, I. Protein organic chemistry and applications for labeling and engineering in live-cell systems. *Angew. Chem. Int. Ed. Engl.* **2013,** *52* (15), 4088-4106.

(3) Bird, R. E.; Lemmel, S. A.; Yu, X.; Zhou, Q. A. Bioorthogonal Chemistry and Its Applications. *Bioconjug. Chem.* **2021,** *32* (12), 2457-2479.

(4) Rigolot, V.; Biot, C.; Lion, C. To View Your Biomolecule, Click inside the Cell. *Angew. Chem. Int. Ed. Engl.* **2021,** *60* (43), 23084-23105.

(5) Kozma, E.; Demeter, O.; Kele, P. Bio-orthogonal Fluorescent Labelling of Biopolymers through Inverse-Electron-Demand Diels–Alder Reactions. *ChemBioChem* **2017,** *18* (6), 486-501.

(6) Kim, E.; Koo, H. Biomedical applications of copper-free click chemistry: in vitro, in vivo, and ex vivo. *Chem. Sci.* **2019,** *10* (34), 7835-7851.

(7) Battigelli, A.; Almeida, B.; Shukla, A. Recent Advances in Bioorthogonal Click Chemistry for Biomedical Applications. *Bioconjug. Chem.* **2022,** *33* (2), 263-271.

(8) Nguyen, S. S.; Prescher, J. A. Developing bioorthogonal probes to span a spectrum of reactivities. *Nat. Rev. Chem.* **2020,** *4* (9), 476-489.

(9) Scinto, S. L.; Bilodeau, D. A.; Hincapie, R.; Lee, W.; Nguyen, S. S.; Xu, M. H.; Ende, C. W. A.; Finn, M. G.; Lang, K.; Lin, Q.; Pezacki, J. P.; Prescher, J. A.; Robillard, M. S.; Fox, J. M. Bioorthogonal chemistry. *Nat. Rev. Methods Primers* **2021,** *1* (1).

(10) Deb, T.; Tu, J. L.; Franzini, R. M. Mechanisms and Substituent Effects of Metal-Free Bioorthogonal Reactions. *Chem. Rev.* **2021,** *121* (12), 6850-6914.

(11) Agard, N. J.; Prescher, J. A.; Bertozzi, C. R. A Strain-Promoted [3 + 2] Azide–Alkyne Cycloaddition for Covalent Modification of Biomolecules in Living Systems. *J. Am. Chem. Soc.* **2004,** *126* (46), 15046-15047.

(12) Dommerholt, J.; Rutjes, F. P. J. T.; van Delft, F. L. Strain-Promoted 1,3-Dipolar Cycloaddition of Cycloalkynes and Organic Azides. *Top. Curr. Chem.* **2016,** *374* (2), 16.

(13) Ning, X. H.; Temming, R. P.; Dommerholt, J.; Guo, J.; Ania, D. B.; Debets, M. F.; Wolfert, M. A.; Boons, G. J.; van Delft, F. L. Protein Modification by Strain-Promoted Alkyne-Nitrone Cycloaddition. *Angew. Chem. Int. Ed. Engl.* **2010,** *49* (17), 3065-3068.

(14) Jawalekar, A. M.; Reubsaet, E.; Rutjes, F. P. J. T.; van Delft, F. L. Synthesis of isoxazoles by hypervalent iodine-induced cycloaddition of nitrile oxides to alkynes. *Chem. Commun.* **2011,** *47* (11), 3198-3200.

(15) Sanders, B. C.; Friscourt, F.; Ledin, P. A.; Mbua, N. E.; Arumugam, S.; Guo, J.; Boltje, T. J.; Popik, V. V.; Boons, G.-J. Metal-Free Sequential [3 + 2]-Dipolar Cycloadditions using Cyclooctynes and 1,3-Dipoles of Different Reactivity. *J. Am. Chem. Soc.* **2011,** *133* (4), 949-957.

(16) Knall, A.-C.; Slugovc, C. Inverse electron demand Diels–Alder (iEDDA)-initiated conjugation: a (high) potential click chemistry scheme. *Chem. Soc. Rev.* **2013,** *42* (12), 5131-5142.

(17) Oliveira, B. L.; Guo, Z.; Bernardes, G. J. L. Inverse electron demand Diels-Alder reactions in chemical biology. *Chem. Soc. Rev.* **2017,** *46* (16), 4895-4950.

(18) Blackman, M. L.; Royzen, M.; Fox, J. M. Tetrazine ligation: fast bioconjugation based on inverse-electron-demand Diels-Alder reactivity. *J. Am. Chem. Soc.* **2008,** *130* (41), 13518-13519.

(19) Knall, A. C.; Hollauf, M.; Slugovc, C. Kinetic studies of inverse electron demand Diels-Alder reactions (iEDDA) of norbornenes and 3,6-dipyridin-2-yl-1,2,4,5-tetrazine. *Tetrahedron Lett.* **2014,** *55* (34), 4763-4766.

(20) Vrabel, M.; Kolle, P.; Brunner, K. M.; Gattner, M. J.; Lopez-Carrillo, V.; de Vivie-Riedle, R.; Carell, T. Norbornenes in inverse electron-demand Diels-Alder reactions. *Chem. Eur. J.* **2013,** *19* (40), 13309-13312.

(21) Patterson, D. M.; Nazarova, L. A.; Xie, B.; Kamber, D. N.; Prescher, J. A. Functionalized Cyclopropenes As Bioorthogonal Chemical Reporters. *J. Am. Chem. Soc.* **2012,** *134* (45), 18638-18643.

(22) Selvaraj, R.; Fox, J. M. trans-Cyclooctene—a stable, voracious dienophile for bioorthogonal labeling. *Curr. Opin. Chem. Biol.* **2013,** *17* (5), 753-760.

(23) Chen, W. X.; Wang, D. Z.; Dai, C. F.; Hamelberg, D.; Wang, B. H. Clicking 1,2,4,5-tetrazine and cyclooctynes with tunable reaction rates. *Chem. Commun.* **2012,** *48* (12), 1736-1738.

(24) Kamber, D. N.; Liang, Y.; Blizzard, R. J.; Liu, F.; Mehl, R. A.; Houk, K. N.; Prescher, J. A. 1,2,4-Triazines Are Versatile Bioorthogonal Reagents. *J. Am. Chem. Soc.* **2015,** *137* (26), 8388-8391.

(25) Horner, K. A.; Valette, N. M.; Webb, M. E. Strain-Promoted Reaction of 1,2,4-Triazines with Bicyclononynes. *Chem. Eur. J.* **2015,** *21* (41), 14376-14381.

(26) Kamber, D. N.; Nguyen, S. S.; Liu, F.; Briggs, J. S.; Shih, H. W.; Row, R. D.; Long, Z. G.; Houk, K. N.; Liang, Y.; Prescher, J. A. Isomeric triazines exhibit unique profiles of bioorthogonal reactivity. *Chem. Sci.* **2019,** *10* (39), 9109-9114.

(27) Siegl, S. J.; Dzijak, R.; Vazquez, A.; Pohl, R.; Vrabel, M. The discovery of pyridinium 1,2,4-triazines with enhanced performance in bioconjugation reactions. *Chem. Sci.* **2017,** *8* (5), 3593-3598.

(28) Liu, F.; Liang, Y.; Houk, K. N. Theoretical elucidation of the origins of substituent and strain effects on the rates of Diels-Alder reactions of 1,2,4,5-tetrazines. *J. Am. Chem. Soc.* **2014,** *136* (32), 11483-11493.

(29) Kämpchen, T.; Massa, W.; Overheu, W.; Schmidt, R.; Seitz, G. Zur Kenntnis von Reaktionen des 1,2,4,5-Tetrazin-3,6-dicarbonsäure-dimethylesters mit Nucleophilen. *Chem. Ber.* **1982,** *115* (2), 683-694.

(30) Svatunek, D.; Wilkovitsch, M.; Hartmann, L.; Houk, K. N.; Mikula, H. Uncovering the Key Role of Distortion in Bioorthogonal Tetrazine Tools That Defy the Reactivity/Stability Trade-Off. *J. Am. Chem. Soc.* **2022,** *144* (18), 8171-8177.

(31) Zhang, H.; Trout, W. S.; Liu, S.; Andrade, G. A.; Hudson, D. A.; Scinto, S. L.; Dicker, K. T.; Li, Y.; Lazouski, N.; Rosenthal, J.; Thorpe, C.; Jia, X.; Fox, J. M. Rapid Bioorthogonal Chemistry Turn-on through Enzymatic or Long Wavelength Photocatalytic Activation of Tetrazine Ligation. *J. Am. Chem. Soc.* **2016,** *138* (18), 5978-5983.

(32) Jemas, A.; Xie, Y.; Pigga, J. E.; Caplan, J. L.; Am Ende, C. W.; Fox, J. M. Catalytic Activation of Bioorthogonal Chemistry with Light (CABL) Enables Rapid, Spatiotemporally Controlled Labeling and No-Wash, Subcellular 3D-Patterning in Live Cells Using Long Wavelength Light. *J. Am. Chem. Soc.* **2022,** *144* (4), 1647-1662.

(33) Liu, L. P.; Zhang, D. Y.; Johnson, M.; Devaraj, N. K. Light-activated tetrazines enable precision live-cell bioorthogonal chemistry. *Nat. Chem.* **2022,** *14* (9), 1078-1085.

(34) Chen, B.-M.; Cheng, T.-L.; Roffler, S. R. Polyethylene Glycol Immunogenicity: Theoretical, Clinical, and Practical Aspects of Anti-Polyethylene Glycol Antibodies. *ACS Nano* **2021,** *15* (9), 14022-14048.

(35) Yang, N. J.; Hinner, M. J., Getting Across the Cell Membrane: An Overview for Small Molecules, Peptides, and Proteins. In *Site-Specific Protein Labeling: Methods and Protocols*, Gautier, A.; Hinner, M. J., Eds. Springer New York: New York, NY, 2015; pp 29-53.

(36) Dzijak, R.; Galeta, J.; Vazquez, A.; Kozak, J.; Matousova, M.; Fulka, H.; Dracinsky, M.; Vrabel, M. Structurally Redesigned Bioorthogonal Reagents for Mitochondria-Specific Prodrug Activation. *JACS Au* **2021,** *1* (1), 23-30.

(37) Chupakhin, O. N.; Rudakov, B. V.; Alexeev, S. G.; Shorshnev, S. V.; Charushin, V. N. 1-Alkyl-1,2,4-triazinium Ylides as 1,3-Dipoles in a Cycloaddition Reaction with Diethyl Acetylenedicarboxylate. *Mendeleev Commun.* **1992,** *2* (3), 85-86.

(38) Galeta, J.; Šlachtová, V.; Dračínský, M.; Vrabel, M. Regio- and Diastereoselective 1,3-Dipolar Cycloadditions of 1,2,4-Triazin-1-ium Ylides: a Straightforward Synthetic Route to Polysubstituted Pyrrolo[2,1-f][1,2,4]triazines. *ACS Omega* **2022,** *7* (24), 21233-21238.

(39) Mochulskaya, N. N.; Andreiko, A. A.; Charushin, V. N.; Shulgin, B. V.; Raikov, D. V.; Solomonov, V. I. Intermolecular and intramolecular cycloaddition reactions of 1-ethyl-1,2,4-triazinium salts with alkynes. *Mendeleev Commun.* **2001,** (1), 19-21.

(40) Meijer, A.; Otto, S.; Engberts, J. B. F. N. Effects of the hydrophobicity of the reactants on Diels-Alder reactions in water. *J. Org. Chem.* **1998,** *63* (24), 8989-8994.

(41) Svatunek, D.; Houszka, N.; Hamlin, T. A.; Bickelhaupt, F. M.; Mikula, H. Chemoselectivity of Tertiary Azides in Strain-Promoted Alkyne-Azide Cycloadditions. *Chem. Eur. J.* **2019,** *25* (3), 754-758.

(42) Hu, Y.; Schomaker, J. M. Recent Developments and Strategies for Mutually Orthogonal Bioorthogonal Reactions. *ChemBioChem* **2021,** *22* (23), 3254-3262.

(43) Smeenk, M. L. W. J.; Agramunt, J.; Bonger, K. M. Recent developments in bioorthogonal chemistry and the orthogonality within. *Curr. Opin. Chem. Biol.* **2021,** *60*, 79-88.

(44) La-Venia, A.; Dzijak, R.; Rampmaier, R.; Vrabel, M. An Optimized Protocol for the Synthesis of Peptides Containing trans-Cyclooctene and Bicyclononyne Dienophiles as Useful Multifunctional Bioorthogonal Probes. *Chem. Eur. J.* **2021,** *27* (54), 13632-13641.

(45) Klima, M.; Toth, D. J.; Hexnerova, R.; Baumlova, A.; Chalupska, D.; Tykvart, J.; Rezabkova, L.; Sengupta, N.; Man, P.; Dubankova, A.; Humpolickova, J.; Nencka, R.; Veverka, V.; Balla, T.; Boura, E. Structural insights and in vitro reconstitution of membrane targeting and activation of human PI4KB by the ACBD3 protein. *Sci. Rep.* **2016,** *6*, 23641.

(46) Goldstein, I. J.; Poretz, R. D., Isolation, physicochemical characterization, and carbohydrate-binding specificity of lectins. In *The Lectins. Properties, Functions, and Applications in Biology and Medicine.*, Liener, I. E.; Sharon, N.; Goldstein, I. J., Eds. Elsevier: 1986; Vol. 32, pp 33-247.

(47) Siegl, S. J.; Galeta, J.; Dzijak, R.; Dracinsky, M.; Vrabel, M. Bioorthogonal Fluorescence Turn-On Labeling Based on Bicyclononyne-Tetrazine Cycloaddition Reactions that Form Pyridazine Products. *ChemPlusChem* **2019,** *84* (5), 493-497.

(48) Murphy, M. P. Targeting lipophilic cations to mitochondria. *BBA-Bioenergetics* **2008,** *1777* (7-8), 1028-1031.

(49) Karver, M. R.; Weissleder, R.; Hilderbrand, S. A. Synthesis and evaluation of a series of 1,2,4,5-tetrazines for bioorthogonal conjugation. *Bioconjug. Chem.* **2011,** *22* (11), 2263-2270.

(50) Murrey, H. E.; Judkins, J. C.; Am Ende, C. W.; Ballard, T. E.; Fang, Y.; Riccardi, K.; Di, L.; Guilmette, E. R.; Schwartz, J. W.; Fox, J. M.; Johnson, D. S. Systematic Evaluation of Bioorthogonal Reactions in Live Cells with Clickable HaloTag Ligands: Implications for Intracellular Imaging. *J. Am. Chem. Soc.* **2015,** *137* (35), 11461-11475.

(51) Bertheussen, K.; van de Plassche, M.; Bakkum, T.; Gagestein, B.; Ttofi, I.; Sarris, A. J. C.; Overkleeft, H. S.; van der Stelt, M.; van Kasteren, S. I. Live-Cell Imaging of Sterculic Acid-a Naturally Occurring 1,2-Cyclopropene Fatty Acid-by

Bioorthogonal Reaction with Turn-On Tetrazine-Fluorophore Conjugates. *Angew. Chem. Int. Ed. Engl.* **2022,** *61* (38), e202207640.

(52) Galeta, J.; Dzijak, R.; Oboril, J.; Dracinsky, M.; Vrabel, M. A Systematic Study of Coumarin-Tetrazine Light-Up Probes for Bioorthogonal Fluorescence Imaging. *Chem. Eur. J.* **2020,** *26* (44), 9945-9953.

Table of Contents artwork